High Frequency Active Distortion Cancellation

Balázs Varga, György Orosz
Budapest University of Technology and Economics
Department of Measurement and Information Systems
Budapest, Hungary
Email: bvarga92@gmail.com, orosz@mit.bme.hu

***Abstract*—This paper presents a signal processing method for cancelling spurious distortion products in high frequency bandpass signals. The proposed method uses a direct-conversion demodulator to transpose the signal to baseband, and a resonator-based observer to determine the harmonic content of the baseband signal. Based on the observed parameters, the algorithm generates an appropriate signal that is converted back to the carrier frequency and subtracted from the original signal, in order to suppress the distortion products. The method is illustrated by simulations and an experimental implementation.**

***Index Terms*—active distortion cancellation, IQ modulation, digital signal processing**

I. Introduction

Power amplifiers and other active electrical devices often exhibit nonlinearity, which causes spectral components that are not present in the input signal to appear in the output signal. These unwanted distortion products may adversely affect the operation in several applications where high spectral purity is required, such as wireless communications and high-precision instrumentation. In these cases, the effects of nonlinearities must be minimized so that the output signal can be as free of spurious spectral contents as possible.

Methods for compensating nonlinearities can be divided into two major categories: passive and active. *Passive* approaches utilize no on-line adaptation, the distortion compensation mechanism is designed along with the entire system, and is not changed during operation. The simplest example is filtering the signal with an analog or digital bandpass filter tuned to fixed frequencies. A more advanced approach involves the identification of the transfer function and the pre-distortion of the input signal according to the inverse of the identified function [1]. The obvious disadvantage of these passive methods is the necessary presupposition of long-term stability – if the transfer function changes during operation, the compensation will no longer work properly.

In *active* distortion cancellation, nonlinearities are compensated by a digital control loop which adds an appropriate signal to the input or the output of the system, suppressing unwanted frequency components, and making the resulting response appear linear [2]. With active distortion cancellation, it is not necessary to make assumptions about the nature of the nonlinearity at design time; the transfer function is adaptively identified and compensated during operation.

However, active methods are not without drawbacks either. Fig. 1 shows two possible arrangements of an active distortion cancelling system. The addition of the compensating signal can be performed at the input or the output of the nonlinear system. In the former case, the nonlinear system is part of the control loop, which may have detrimental effects on the stability and dynamical properties. On the other hand, if the summation takes place at the output of a power amplifier, the large signal amplitudes may present a practical challenge [2].

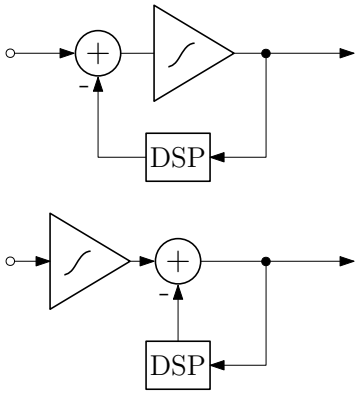

Fig. 1. Summation at input vs. output.

This paper is structured as follows. Section II describes an algorithm for determining the amplitude and phase of the distortion products. In Section III, a digital controller is introduced that can be used in active distortion cancelling systems, and a method is proposed by which this controller can be extended to work on high frequency signals. The described methods are illustrated with numerical simulations in Section IV. Section V highlights some potential difficulties that may rise in practical implementations. In Section VI, an experimental implementation of high frequency active distortion cancellation is presented, along with measurement results. Finally, Section VII concludes the paper.

II. Detection of Distortion Products

Let us consider the nth sample of the signal y as a scalar product of a basis vector $\mathbf{c}_n^T$ and a state vector $\mathbf{x}_n$:

$$y_n = \mathbf{c}_n^T \mathbf{x}_n \tag{1}$$

In the case of the Discrete Fourier Transform (DFT), let $\mathbf{c}_n$ be the nth sample of the set of DFT basis functions:

$$\mathbf{c}_n = [c_{k,n}] = e^{j\omega_k n}, k = -L \dots L \tag{2}$$

$$\omega_{-k} = -\omega_k \tag{3}$$

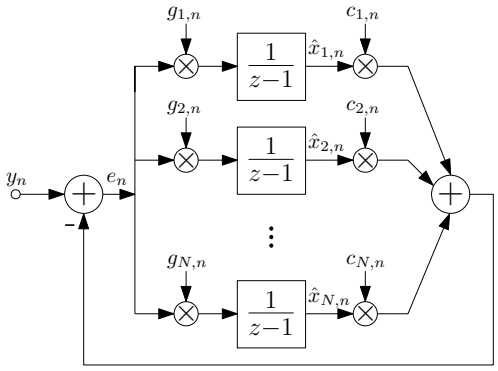

Fig. 2. The resonator-based observer.

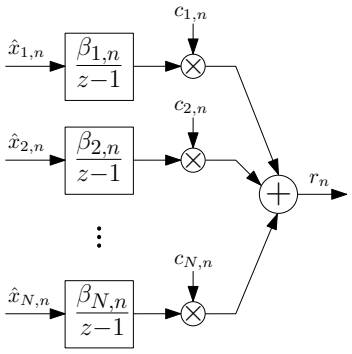

Fig. 3. Traditional controller.

The resonator-based observer (RBO) – introduced and thoroughly analysed in [3] and shown in Fig. 2 – is described by the following equations:

$$\hat{\mathbf{x}}_{n+1} = \hat{\mathbf{x}}_n + \mathbf{g}_n e_n \tag{4}$$

$$e_n = y_n - \mathbf{c}_n^T \hat{\mathbf{x}}_n \tag{5}$$

$$\mathbf{g}_n = [g_{k,n}] = \frac{1}{N} \bar{c}_{k,n} \tag{6}$$

where $\hat{\mathbf{x}}_n$ is the estimated state vector and $N = 2L + 1$. If all equations (1)-(6) are satisfied, the resonator poles are arranged uniformly on the unit circle, and the observer performs a Recursive Discrete Fourier Transform (RDFT) – the estimated state vector $\mathbf{x}_n$ contains the DFT coefficients of y, at frequencies corresponding to the resonator channels [2].

In practice however, usually not all resonator channels need to be realised. In this case, (6) becomes:

$$\mathbf{g}_n = [g_{k,n}] = \alpha \bar{c}_{k,n} \tag{7}$$

where $0 < \alpha < \frac{1}{N}$ is a common convergence parameter, chosen to be small enough to ensure stability. Furthermore, the fundamental frequency f_1 (ω_1) might change over time, or it might be unknown. In such cases, the resonator frequencies can be adaptively tuned to coincide with the harmonics of the input signal [4].

In an active distortion cancelling application, the resonator-based observer can be used to determine the amplitude and phase of the distortion products. The RBO has the following advantages over traditional DFT implementations:

- A current estimate of $\mathbf{x}$ is always available – as opposed to a blockwise DFT implementation.
- Only the necessary resonator channels need to be realised,
- which also allows faster computation.

III. Control Loop

A. Traditional control loop

When the RBO has reached steady state, the error signal is zero and the output follows the input. This feature can be utilized to construct a resonator-based controller, shown in Fig. 3 [2]. The controller contains resonator channels at frequencies that are to be cancelled. The inputs are the corresponding coefficients observed by the RBO. Therefore, if the controller output r_n is subtracted from the input signal y_n, the resulting signal will no longer contain components at the frequencies of the controller channels – assuming the algorithm converges.

In the case when there are only linear systems in the control loop, convergence can be ensured by the appropriate choice of parameters

$$\beta_{k,n} = \frac{\beta}{H(z_k)} \tag{8}$$

where β is a convergence parameter and $H(z_k)$ is the transfer function from the output of the controller to the input of the system, evaluated at the kth frequency [5]. $H(z_k)$ generally cannot be calculated, therefore it has to be measured prior to the beginning of operation. This can be done automatically: the controller generates a sinusoidal signal of the desired frequency, and the RBO observes the corresponding coefficient at the input [2].

When nonlinearities are present in the control loop, stability analysis becomes complicated. However, practical experiments show that the same linear approach works in the majority of these cases as well [2].

B. High frequency control loop

According to the sampling theorem, if a signal contains no frequencies higher than f_B, and it is sampled at a rate of at least $2f_B$, then it can be perfectly reconstructed from its samples. Unfortunately, for high frequency signals – such as those used in wireless communications – blindly applying this rule would necessitate very high sampling rates and computational requirements.

However, different approaches exist for signals with narrow bandwidth that are converted up to a high carrier frequency (also called bandpass, passband, non-baseband or narrowband signals) [6], [7]. In this paper, the method known as IQ modulation is described.

Let us consider the high frequency sinusoidal signal

$$y(t) = A\cos(\omega_c t + \varphi) = \frac{A}{2}\left[e^{j(\omega_c t+\varphi)} + e^{-j(\omega_c t+\varphi)}\right] \tag{9}$$

The spectrum of a real-valued signal always satisfies the Hermitian property – i.e. $Y(-\omega) = \overline{Y(\omega)}$. Multiplication by

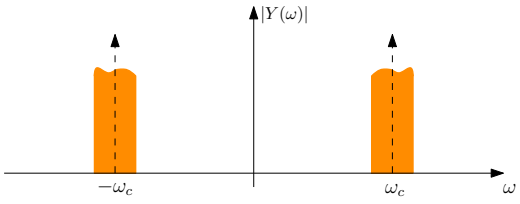

Fig. 4. Bandpass signal.

a complex exponential corresponds to the linear translation of the spectrum and yields a complex-valued signal:

$$\begin{aligned} v(t) &= y(t)e^{-j\omega_0 t} = \\ &= y(t)\cos(\omega_0 t) - jy(t)\sin(\omega_0 t) = \\ &= \frac{A}{2}e^{j((\omega_c-\omega_0)t+\varphi)} + \frac{A}{2}e^{-j((\omega_c+\omega_0)t+\varphi)} \end{aligned} \tag{10}$$

Naturally, a complex-valued signal cannot be realised, however, its real and imaginary part can individually exist as physical signals. If they are digitised separately, then the complex signal can be computationally constructed. Taking into account the anti-aliasing lowpass filters of the analog-to-digital converters (ADCs), and assuming that ω_0 is chosen to be sufficiently close to ω_c, the complex signal becomes

$$v_f(t) = \frac{A}{2}e^{j((\omega_c-\omega_0)t+\varphi)} \tag{11}$$

The filtered complex signal $v_f(t)$ still carries all amplitude and phase information of $y(t)$, but its spectrum has been shifted to the left by ω_0 and the resulting high-frequency component has been omitted. An RBO with a single resonator channel at $\omega_c - \omega_0$ can be used to determine the amplitude and phase of $v_f(t)$, and therefore also of $y(t)$.

The same principle can be used to generate high frequency signals. Let us consider the low frequency complex signal

$$w(t) = Ae^{j(\omega t+\varphi)} \tag{12}$$

The real and imaginary part of $w(t)$ can be individually generated and multiplied by other sinusoidal signals:

$$\begin{aligned} r(t) &= \mathrm{Re}\{w(t)\}\cos(\omega_0 t) - \mathrm{Im}\{w(t)\}\sin(\omega_0 t) = \\ &= A\cos(\omega t+\varphi)\cos(\omega_0 t) - A\sin(\omega t+\varphi)\sin(\omega_0 t) = \\ &= A\cos((\omega+\omega_0)t+\varphi) \end{aligned} \tag{13}$$

Similarly as before, the high frequency real signal $r(t)$ retained the amplitude and phase of its low frequency complex representation $w(t)$.

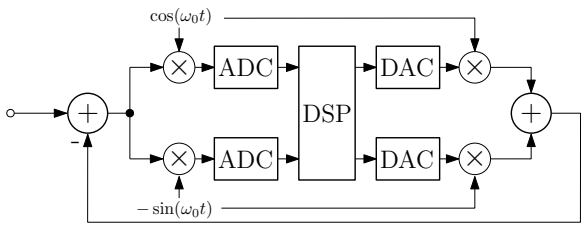

Fig. 5. High frequency controller.

Fig. 5 shows how the method of IQ modulation[1] can be used to extend the traditional distortion cancelling system to work on high frequency signals.

IV. Simulation Results

The high frequency distortion cancelling arrangement shown in Fig. 5 was simulated in MATLAB. The aim was to suppress a single sinusoidal signal with a frequency of $f_c = 110\,\mathrm{kHz}$. The local IQ signals were generated with $f_0 = 100\,\mathrm{kHz}$, resulting in $10\,\mathrm{kHz}$ baseband signals. The complex signal introduced in (11) was assembled and an RBO was applied to it. Then, the control loop was created according to Fig. 5.

The simulation results are shown in figures 6 and 7. The algorithm clearly converges and successfully generates an output signal ($\mathrm{RF_{out}}$) that cancels out the input signal ($\mathrm{RF_{in}}$).

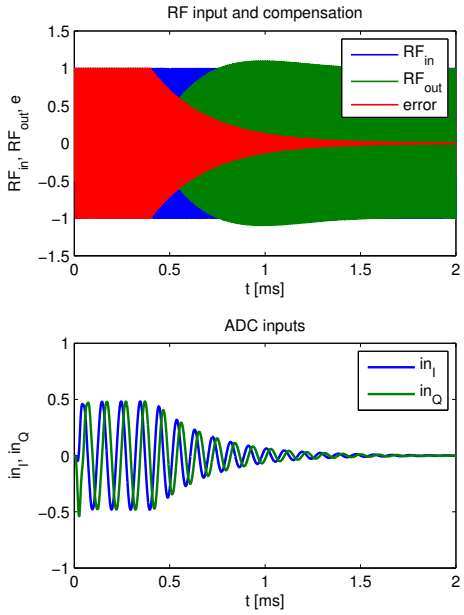

Fig. 6. High frequency (top) and downconverted signals (bottom) at the beginning of the cancellation. The controller is turned on at $0.4\,\mathrm{ms}$.

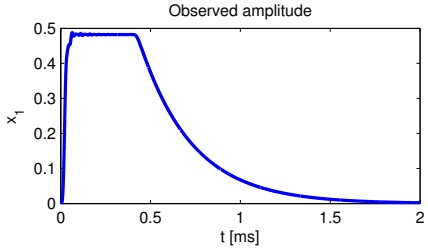

Fig. 7. Magnitude of the estimated state variable $\hat{x}_1$.

[1]The name IQ modulation originates from the fact that the local oscillator produces two signals with a 90 degree phase shift between them: one is often referred to as the in-phase (I) signal, and the other as the quadrature (Q) signal.

V. Implementation issues

Thus far, the in-phase and quadrature signal paths have been assumed perfectly identical. In reality however, imbalances such as offset and gain errors are present. Taking these into account on the downconversion (input) side, (10) becomes:

$$\begin{aligned}\tilde{v}_1(t) &= (y(t)+C)\cos(\omega_0 t) - j\,(y(t)+D)\sin(\omega_0 t) = \\ &= v(t) + C\cos(\omega_0 t) - jD\sin(\omega_0 t) \qquad (14)\\ \tilde{v}_2(t) &= y(t)\,(\cos(\omega_0 t)+C) - jy(t)\,(\sin(\omega_0 t)+D) = \\ &= v(t) + Cy(t) - jDy(t) \qquad (15)\\ \tilde{v}_3(t) &= (1+\epsilon)\,y(t)\cos(\omega_0 t) - jy(t)\sin(\omega_0 t) = \\ &= v(t) + \epsilon y(t)\cos(\omega_0 t) \qquad (16)\end{aligned}$$

As can be seen from (14) and (15), offset errors cause high frequency components to appear, which are of no particular concern, since these are eliminated by the lowpass filters of the ADCs. On the other hand, the gain error results in baseband components, which are sampled by the ADCs.

Similarly, on the upconversion (output) side, (13) becomes:

$$\begin{aligned}\tilde{r}_1(t) &= (\mathrm{Re}\{w(t)\}+C)\cos(\omega_0 t) - \\ &\quad - (\mathrm{Im}\{w(t)\}+D)\sin(\omega_0 t) = \\ &= r(t) + C\cos(\omega_0 t) - D\sin(\omega_0 t) \qquad (17)\\ \tilde{r}_2(t) &= \mathrm{Re}\{w(t)\}(\cos(\omega_0 t)+C) - \\ &\quad - \mathrm{Im}\{w(t)\}(\sin(\omega_0 t)+D) = \\ &= r(t) + AC\cos(\omega t+\varphi) - AD\sin(\omega t+\varphi) \qquad (18)\\ \tilde{r}_3(t) &= (1+\epsilon)\,\mathrm{Re}\{w(t)\}\cos(\omega_0 t) - \\ &\quad - \mathrm{Im}\{w(t)\}\sin(\omega_0 t) = \\ &= \left(1+\frac{\epsilon}{2}\right) r(t) + \frac{A\epsilon}{2}\cos((\omega_0-\omega)t-\varphi) \qquad (19)\end{aligned}$$

In this case, all errors have significant effect on the output signal. A simple way to eliminate these effects is to numerically compensate the errors by the multiplication and addition of appropriate constants – which can be determined via measurement or heuristic (e.g. tune the parameters until the output spectrum is sufficiently pure). This approach proved to be adequate in the experiment presented in Section VI.

VI. Experimental Results

To experimentally illustrate the viability of the described concepts, a high frequency distortion cancelling system prototype was constructed that closely matches the diagram shown in Fig. 5. In our setup, all computation was done by an Analog Devices ADSP-21364 digital signal processor. For the two ADC and two DAC channels, an AD73322L audio codec was used. The IQ signal pair was generated by an AD9854 direct digital synthesizer (DDS) chip designed specifically for this application. The signal multiplications were carried out by four AD835 analog multipliers.

Similarly as in Section IV, the aim was to suppress a high frequency sinusoidal signal. In the measurements presented here, the frequency of the input signal was 101 kHz, and the local oscillator was set to 100 kHz, resulting in 1 kHz baseband signals, which were then sampled by the codec at 64 kHz.

Fig. 8 shows that over 50 dB suppression was achieved. In Fig. 9, the convergence of the algorithm can be observed.

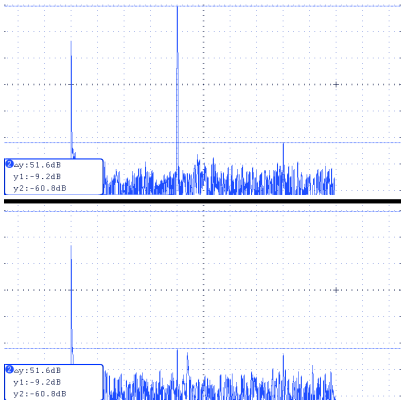

Fig. 8. Output spectrum without (top) and with (bottom) the controller in operation. Horizontal scale 25 kHz/div.

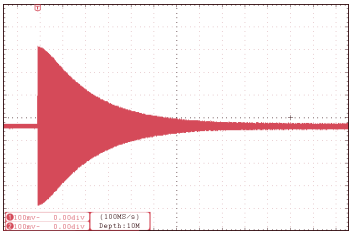

Fig. 9. Settling of the output after applying a 101 kHz signal to the input. Horizontal scale 5 ms/div. Settling time approximately 50 milliseconds.

VII. Conclusion

In this paper, the concept of a high frequency active distortion cancelling system was introduced. The mathematical background was explored and illustrated with simulations, as well as a working prototype. Some practical difficulties were examined and a possible solution was proposed. However, further research should focus on overcoming these issues.

References

[1] M. K. Nezami, "Fundamentals of power amplifier linearization using digital pre-distortion," High Frequency Electronics, pp. 54–59 , September 2004.

[2] L. Sujbert, B. Vargha, "Active distortion cancelation of sinusoidal sources," Proceedings of the IEEE Instrumentation and Measurement Technology Conference, May 2004, Como, Italy, pp. 322–326.

[3] G. Péceli, "A common structure for recursive discrete transforms," IEEE Transactions on Circuits and Systems, vol. CAS-33, pp. 1035–36, October 1986.

[4] F. Nagy, "Measurement of signal parameters using nonlinear observers," IEEE Transactions on Instrumentation and Measurement, vol. IM-41 no. 1, pp. 152–155, February 1992.

[5] L. Sujbert, G. Péceli, "Periodic noise cancelation using resonator based controller," 1997 Int. Symp. on Active Control of Sound and Vibration, ACTIVE 97, pp. 905–916, Budapest, Hungary, August 1997.

[6] R. G. Vaughan, N. L. Scott, D. R. White, "The theory of bandpass sampling," IEEE Transactions on Signal Processing, vol. 39 no. 9, pp. 1973–1984, September 1991.

[7] H. Zhou, Y. Zheng, "An efficient quadrature demodulator for medical ultrasound imaging,", Frontiers of Information Technology & Electronic Engineering, vol. 16 no. 4, pp. 301–310, April 2015.